Inorganic Chemistry

ARTICLE

pubs.acs.org/IC

Highly NIR-Emissive Lanthanide Polyselenides

Anna Kornienko,[†] Brian F. Moore,[†] G. Ajith Kumar,[‡] Mei-Chee Tan,[‡] Richard E. Riman,[‡] Mikhail G. Brik,[§] Thomas J. Emge,[†] and John G. Brennan*[,†]

[†]Department of Chemistry and Chemical Biology and [‡]Department of Materials Science and Engineering, Rutgers, The State University of New Jersey, 610 Taylor Road, Piscataway New Jersey 08854-8087, United States

[§]Institute of Physics, University of Tartu, Riia 142, Tartu 51014, Estonia

Supporting Information

ABSTRACT: $Ln(SePh)_3$ (Ln = Ce, Pr, Nd), prepared by reduction of PhSeSePh with elemental Ln and Hg catalyst, reacts with excess elemental Se to give $(py)_{11}Ln_7Se_{21}HgSePh$, an ellipsoidal polyselenide cluster. The molecular structure contains two square arrays of eight- or nine-coordinate Ln fused at one edge to form a V shape that is also capped on the concave side by a centrally located nine-coordinate $(Se_3)pyLn(Se_3)$ and on the convex side by a 2-fold disordered SeHgSePh. The central Ln coordinates to selenido, triselenido, and pyridine ligands, while all other Ln coordinate to selenido, diselenido, triselenido, and pyridine ligands. Thermal treatment of the Pr compound at 650 °C gave Pr_2Se_3 and Pr_3Se_4. NIR emission studies of the Nd compound show four transitions from the excited-state $^4F_{3/2}$ ion to $^4I_{9/2}$, $^4I_{11/2}$, $^4I_{13/2}$, and $^4I_{15/2}$ states. The $^4F_{3/2}$ ion to $^4I_{11/2}$ transition (1075 nm emission) exhibited 43% quantum efficiency. This is the highest quantum efficiency reported for a 'molecular' Nd compound and leads a group of selenide-based clusters that has shown extraordinary quantum efficiency. In terms of efficiency and concentration, these compounds compare favorably with solid-state materials.

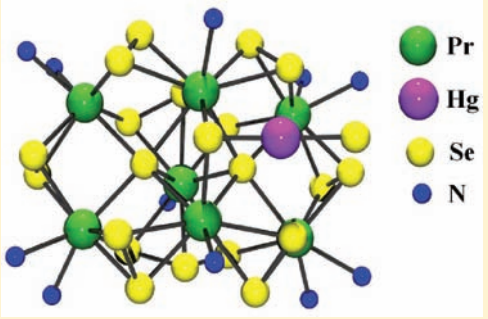

INTRODUCTION

Fundamental studies of materials with ionic lanthanide (Ln, Ln = La−Lu) cations bound to covalent chalcogen (E; E = S, Se, Te) based anions continue to be motivated by the extraordinary NIR emission properties of compounds with Ln−E bonds. Chalcogen-based anions provide a low-phonon energy environment[1−3] that reduces the vibrational relaxation of Ln excited states, and leads to improved quantum efficiencies for both molecular[4] and cluster compounds.[5] Cluster compounds are particularly important because they can deliver increasingly large concentrations of Ln, to the extent that they might actually be useful as optical amplifiers in organic polymer fiber systems.[6]

While Ln cluster chemistry has yet to approach the level of accomplishment set by main group cluster chemists, in terms of either synthetic methodology[7] or defining how material properties evolve with dimension,[8] there is now a better understanding of how Ln, E, and R influence structure−property relationships, and this knowledge can be applied to the rational synthesis of cluster compounds with desirable physical characteristics. With more covalent main group or transition metals, chalcogenido chemistry includes ER, E^{2-}, and EE^{2-} ligands but there is also a significant body of literature describing compounds with polychalcogen[9] ligands (E_n^{2-}; n = 3−12). This field is remarkably diverse and well understood because many of the products are diamagnetic, allowing for detailed NMR investigations into molecular dynamics and reactivity of these covalent compounds.

In contrast, the related polychalcogenide literature of the lanthanide metals is virtually unexplored. The first and smallest example is the organometallic derivative $Cp^*_2Sm(Se_3)SmCp^*_2$[10a] that was trapped as a bimetallic product because the steric stabilization of the Cp* ligands inhibited ligand redistribution processes. This work has also led to the preparation of organometallic clusters with hexanuclear Ln_6Se_x cores encapsulated with substituted Cp ligands.[10b,c]

There are also octanuclear oxoclusters[11] isolated from metathetical reactions of $LnCl_3$ (Ln = Eu,[11a] Gd, Y, Yb[11b]) with $NaSe_x$ (in which the polyselenide ligand is prevented from extensive coordination to Ln by the presence of more electronegative oxo ligands), and there is a group of tetrametallic telluride clusters[12] with TeTe dianions that contain weak interactions with TePh to give what can be described as polytelluride compounds with Te_5Ph^{5-} and Te_9Ph^{9-} ligands.

Polychalcogenide ligands are potentially useful for enhancing the emission properties of lanthanide clusters for a number of reasons. First, as with EPh, E^{2-}, or EE^{2-} ligands, E_n^{2-} provide a low-phonon environment that minimizes vibrational relaxation. Second, with increasingly large numbers of E atoms separating Ln ions one can potentially increase the Ln−Ln distances and lower the propensity for excited-state quenching via an energy migration pathway. Finally, compounds with E_n^{2-} ligands have

Received: July 15, 2011
Published: August 25, 2011

distinct advantages when compared with the other chalcogen-based anions. They are superior to EPh ligands because E_n^{2-} contain no emission quenching C−H moieties, and they will be more soluble than clusters with E^{2-} ligands because the delocalized charge results in weaker Ln−E electrostatic interactions, making Ln−solvent interactions more competitive. For these reasons we elected to investigate whether we could prepare NIR emissive Ln clusters with polyselenide ligands, and we here describe our initial results.

EXPERIMENTAL SECTION

General Methods. All syntheses were carried out under ultrapure nitrogen (Welco Praxair) using conventional drybox or Schlenk techniques. Pyridine (Aldrich) was purified with a dual-column Solv-Tek solvent purification system and collected immediately prior to use. PhSeSePh was purchased and recrystallized from hexane. Ln (Strem) and mercury (Aldrich) metals were purchased and used as received. Melting points were recorded in sealed capillaries and are uncorrected. FTIR spectra were recorded on a Thermo Nicolet Avatar 360 FTIR spectrometer from 4000 to 450 cm^{-1} as Nujol mulls on CsI plates. Elemental analyses were performed by Quantitative Technologies, Inc. (Whitehouse, NJ).

*Synthesis of (py)$_{11}$Ce$_7$(μ_5-Se)$_2$(μ_3-Se)(μ_2-Se$_2$)$_5$(μ_3-Se$_2$)(μ_4-Se$_3$)$_2$Hg(SePh)·7py (**1**).* Ce (0.28 g, 2.0 mmol), diphenyl diselenide (0.94 g, 3.0 mmol), and Hg (0.056 g, 0.29 mmol) were combined in pyridine (50 mL). The mixture was stirred for 4 h until all the metal was dissolved to give a bright yellow solution. Elemental Se (0.45 g, 5.7 mmol) was added, and in 20 min the black/red solution was filtered and layered with hexanes (5.0 mL) to give dark red needles (1.1 g, 88% based on Ln) that do not melt but turn brown at 180 °C and then black-gray at 210 °C. Anal. Calcd for $C_{96}H_{95}N_{18}Se_{22}HgCe_7$: C, 26.1; H, 2.17; N, 5.71. Found: C, 25.8; H, 2.09; N, 5.11. UV−vis (THF): 430 ($\varepsilon = 1.1 \times 10^3$) nm. IR: 3077 (s), 2926 (w), 2854 (m), 2728 (s), 2365 (s), 2345 (s), 1943 (s), 1844 (s), 1612 (s), 1580 (m), 1461 (m), 1438 (m), 1377 (m), 1306 (s), 1260 (s), 1215 (s), 1144 (s), 1068 (s), 1030 (s), 990 (s), 744 (s), 701 (m) cm^{-1}. Crystal data of $C_{101}H_{100}HgN_{19}Ce_7Se_{22}$ (**1**): fw = 4498.55, orthorhombic, *Pbcn*, a = 31.183(4), b = 34.912(5), c = 12.7680(19) Å, V = 13900(3) Å^3, D_c = 2.150 g cm^{-3}, μ(Mo Kα) = 9.149 mm^{-1}. Measurements were made on a Bruker SMART APEX CCD area detector at 100(2) K with graphite-monochromated Mo Kα radiation (λ = 0.71073 Å).

*Synthesis of (py)$_{11}$Pr$_7$(μ_5-Se)$_2$(μ_3-Se)(μ_2-Se$_2$)$_5$(μ_3-Se$_2$)(μ_4-Se$_3$)$_2$Hg(SePh)·7py (**2**).* Pr (0.28 g, 2.0 mmol), diphenyl diselenide (0.94 g, 3.0 mmol), and Hg (0.056 g, 0.29 mmol) were combined in pyridine (50 mL). The mixture was stirred for 4 h until all the metal was dissolved to give a deep green solution. Elemental Se (0.45 g, 5.7 mmol) was added, and in 20 min the black/red solution was filtered and layered with hexanes (5.0 mL) to give dark red long needles (1.0 g, 82%) that do not melt but turn brown at 185 °C . Anal. Calcd for $C_{96}H_{95}N_{18}Se_{22}HgPr_7$: C, 26.1; H, 2.16; N, 5.70. Found: C, 27.0; H, 3.12; N, 6.08. UV−vis (THF): 440 ($\varepsilon = 1.3 \times 10^3$) nm. IR: 3077 (s), 2914 (w), 2858 (s), 2678 (s), 2365 (s), 2345 (s), 1913 (s), 1862 (s), 1596 (s), 1579 (m), 1461 (m), 1438 (m), 1377 (m), 1305 (s), 1260 (s), 1216 (s), 1144 (s), 1068 (s), 1030 (s), 990 (s), 745 (s), 701 (m) cm^{-1}.

*Synthesis of (py)$_{11}$Nd$_7$(μ_5-Se)$_2$(μ_3-Se)(μ_2-Se$_2$)$_5$(μ_3-Se$_2$)(μ_4-Se$_3$)$_2$Hg(SePh)·7py (**3**).* Nd (0.28 g, 2 mmol), diphenyl diselenide (0.93 g, 3.0 mmol), and Hg (0.056 g, 0.29 mmol) were stirred in pyridine (50 mL) for 12 h to give a deep green solution. Elemental Se (0.45 g, 5.7 mmol) was added, and in 20 min the black/red solution was filtered and layered with hexanes (0.50 mL) to give dark red needles (1.1 g, 86%) that turn deep brown at 182 °C and do not melt below 300 °C Anal. Calcd for $C_{96}H_{95}N_{18}Se_{22}HgNd_7$: C, 26.0; H, 2.15; N, 5.67. Found: C, 25.8; H, 2.09; N, 5.50. UV−vis (THF): 445 ($\varepsilon = 4.2 \times 10^3$) nm. IR: 3171 (s), 2924 (w), 2728 (s), 2670 (s), 2365 (s), 2345 (s), 2035 (s), 1838 (s), 1595 (s), 1561 (s), 1543 (s), 1461 (w), 1438 (m), 1377 (w), 1307 (s), 1262 (w), 1218 (s), 1152 (s), 1069 (s), 991(s), 744 (m), 701(m) cm^{-1}. The ^{1}H NMR spectrum (C_5D_5N, 20 °C) contained resonances from rapidly exchanging free and coordinated pyridine (8.71, 7.56, 7.20 ppm). Crystal data of $C_{101}H_{100}HgN_{19}Nd_7Se_{22}$ (**3**): fw = 4527.39, orthorhombic, *Pbcn*, a = 30.641(6), b = 35.283(7), c = 12.659(2), V = 13685(5) Å^3, D_c = 2.197 g cm^{-3}, μ(Cu Kα) = 28.874 mm^{-1}. Measurements were made on a Bruker SMART APEX CCD area detector at 100(2) K with graphite-monochromated Cu Kα radiation (λ = 1.5418 Å).

Table 1. Summary of Crystallographic Details for 2[a]

compound	**2**
empirical formula	$C_{101}H_{100}HgN_{19}Pr_7Se_{22}$
fw	4504.08
space group	*Pbcn*
a (Å)	30.5993(15)
b (Å)	35.3540(17)
c (Å)	12.6664(6)
V (Å^3)	13703(1)
Z	4
D(calcd) (g/cm^{-3})	2.183
temp. (K)	100(2)
λ (Å)	0.71073
abs coeff (mm^{-1})	9.444
independent reflns [$I > 2\sigma(I)$]	9832 [R(int) = 0.068]
$R(F)$[b] [$I > 2\sigma(I)$]	0.076
$R_w(F^2)$[c] [$I > 2\sigma(I)$]	0.123

[a] Additional crystallographic details are given in the Supporting Information. [b] $R(F) = \Sigma||F_o| - |F_c||/\Sigma|F_o|$; [c] $R_w(F^2) = \{\Sigma[w(F_o^2 - F_c^2)^2]/\Sigma[w(F_o^2)^2]\}^{1/2}$

X-ray Structure Determination. Data for **1**, **2**, and **3** were collected on a Bruker Smart APEX CCD diffractometer with graphite-monochromatized Mo Kα radiation (λ = 0.71073 Å) at 100 K. Crystals were immersed in Paratone oil and examined at low temperatures. The X-ray data for **1** and **3** provided lower resolution structures (Supporting Information) and precise unit cell parameters that verified their structures to be isostructural to that of **2** (Table 1). The X-ray data for **2** were corrected for Lorenz effects and polarization and absorption, the latter by a multiscan (SADABS)[13] method. The structure of **2** was solved by direct methods (SHELXS86).[14] All non-hydrogen atoms were refined (SHELXL97)[15] based upon F_{obs}^2. With one Hg atom per Nd7 and C_2 site symmetry for the cluster, the environment about the general position

dx.doi.org/10.1021/ic201509v |*Inorg. Chem.* 2011, 50, 9184–9190

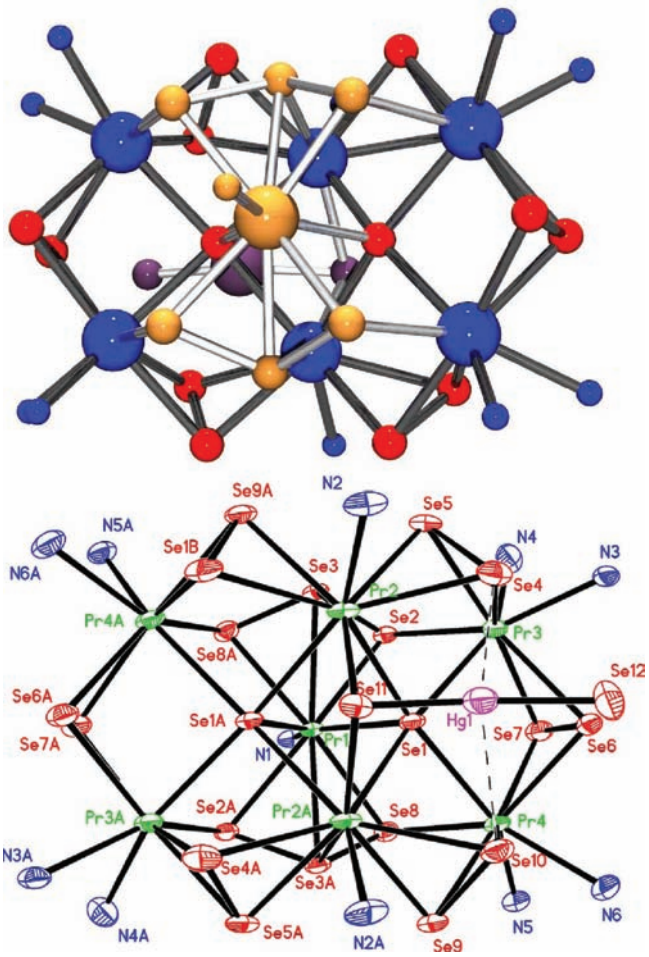

Figure 1. (Top) POV-ray diagram illustrating the dual-capped edge-sharing squares of lanthanide (blue) and diselenide (red), with (Se)Hg(SePh) rear-capping group (violet) and (Se_3)pyLn(Se_3) front-capping group (yellow). (Bottom) ORTEP diagram of non-C atoms in $(py)_{11}Pr_7Se_{21}$(HgSePh), with ellipsoids at the 50% probability level. The view is nearly along the crystallographic 2-fold axis and the Pr(1)−N(1) bond. Selected bond length averages and ranges [Å] for **2**: Pr(9-coord)−Se 3.08(9) [2.97−3.29]; Pr(8-coord)−Se 3.00(6) [2.94−3.11]; Hg(2-coord)−Se 2.46(1) [2.45−2.48]; Hg···Se(dative) 3.14(9) [3.07−3.21]; Pr(9-coord)−N 2.75(4) [2.72−2.80]; Pr(8-coord)−N 2.67(3) [2.63−2.69]; Se−Se (Se_2) 2.38(1) [2.37−2.39]; Se−Se (Se_3) 2.38(1) [2.38−2.39].

of the SeHgSePh group was necessarily disordered and best modeled by placing (then refining with distance restraints) the centrally located (1/2, *y*, 1/4) Se atom of the SeHgSePh group, Se(11), at $\Delta x = 0.006/\Delta z = 0.004$ from the nearby symmetry site. Then, the position and displacement parameters of the SeHgSePh moiety at 50% occupancy were modeled in SHELXL as "PART 1". For "PART 2" of this site, a combination of a selenide ligand, Se(21) near Se(11; $1 - x$, *y*, $1/2 - z$), and pyridine of crystallization all at 50% occupancy was used. Subsequently, SHELXL distance and displacement parameter restraints were used for atoms Se(11) and Se(12) in the final cycles of refinement. All hydrogen atom coordinates were calculated with idealized geometries (SHELXL97). Scattering factors (f_o, f', f'') are as described in SHELXL97. Crystallographic data and final *R* indices for **2** are given in Table 1. An ORTEP diagram[16] for the common structure of **1**, **2**, and **3** is shown in Figure 1 with a selected bond distance summary for **2** given in the figure caption. Complete crystallographic details are given in the Supporting Information.

Scheme 1

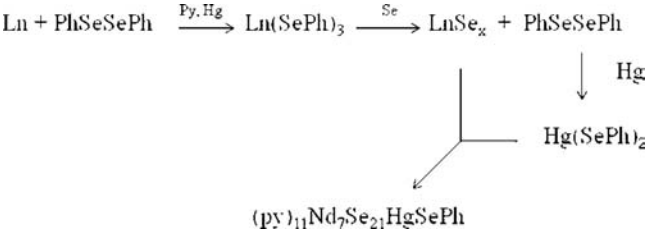

Thermolysis. Crystalline **2** was placed in a quartz tube that was then sealed under vacuum. The end of the tube with the sample was placed in the oven. The temperature of the oven was raised quickly (20 °C/min) until it was stabilized at 650 °C and then was kept at this temperature for 5 h. The other end of the thermolysis tube was kept in liquid nitrogen during the experiment. Black powders formed, and powder diffraction patterns obtained by scanning from 20° to 80° identified the presence of both Pr_2Se_3[17] and Pr_3Se_4[18] phases. The cold part of the tube was washed with acetonitrile and then analyzed by GC/MS spectrometry to identify Ph_2Se as the only volatile product of the reaction.

Spectroscopy. Solution absorption measurements were carried out in THF solution using an integrating sphere of a double-beam spectrophotometer (Perkin-Elmer Lambda 9, Wellesley, MA). The emission spectra of a powdered sample were recorded by exciting the sample with a 0.7 W 800 nm photodiode from B&W Tek (Newark, NJ). The 900−1500 nm emission from the sample was focused onto a 0.55 m monochromator (Jobin Yvon, Triax 550, Edison, NJ) and detected by a thermoelectrically cooled InGaAs detector. The signal was intensified with a lock-in amplifier (SR 850 DSP, Stanford Research System, Sunnyvale, CA) and processed with a computer controlled by the Synerjy commercial software. To measure the decay time, the laser beam was modulated by a chopper and the signal was collected on a digital oscilloscope (TDS 220, 200 MHz, Tektronix, Beaverton, OR). The emission spectra from 1700 to 1900 nm excited at ~800 nm with a 0.7 W laser (BW976, B&W Tek, Newark, NJ) were collected using a FSP920 Edinburgh Instruments spectrometer (Edinburgh Instruments, Livingston, U.K.) that was equipped with a Hamamatsu G5852-23 thermoelectrically cooled shortwave infrared sensitive InGaAs photodiode. The emission data analysis method follows those discussed in our earlier work.[4,5]

RESULTS

Polyselenide compounds of the early lanthanides (Ln = Ce, Pr, Nd) can be prepared in nearly quantitative yield by reaction of in-situ-prepared $Ln(SePh)_3$ (Scheme 1) with elemental Se in pyridine. Reduction of Se leads to the oxidative elimination of $(SePh)_2$, which then reacts with the Hg present as a catalyst to increase the rate of $Ln(SePh)_3$ formation. The resultant mercury chalcogenolate then reacts with the lanthanide polyselenide to cap only one of the two 2-fold symmetry-related sides of the cluster, whose structure was determined by low-temperature single-crystal X-ray diffraction to be $py_{11}Ln_7Se_3(Se_2)_6(Se_3)_2$Hg(SePh) (Scheme 1). This compound was found to be a rather oblong cluster containing a "V"-shaped edge-sharing pair of $Ln_4Se(Se_2)_4$ squares (vide infra), depicted by the blue Ln and red Se in Figure 1(top). The cluster is capped not only on the convex side by (Se)Hg(SePh) (the violet group in the rear in Figure 1(top)) but also on the concave side by a 9-coordinate Ln in the form of (Se_3)pyLn(Se_3) (yellow group in the front in Figure 1(top)). The ORTEP diagram in Figure 1(bottom)

shows the obverse side of Figure 1(top). The centroid of the disordered halves of the selenido of the (Se)Hg(SePh) and the N and Ln atoms of the (Se_3)pyLn(Se_3) are located on a crystallographic 2-fold axis. As required by stoichiometry, only one SeHgSePh is shown in Figure 1. The structures of **1** and **3** have nearly identical unit cells, crystal structures, and molecular structures as those of **2**, within the low-resolution limit of X-ray data collected at 1.00 and 0.95 Å, respectively, for **1** and **3** (see Supporting Information).

The diverse array of chalcogen-based anions that bridge the Ln atoms include selenido, diselenido, and triselenido dianions. The (Se)Hg(SePh) unit contains the only terminal selenolate and exists at either, but not both, of the two sites related by the crystallographic 2-fold axis and alternates at this site with a pyridine molecule of solvation. The choice of site appears to be random, e.g., the ratio of the left-hand site to the right-hand site in Figure 1 is 1:1.

In the molecular structure of **2**, the central Ln is Pr(1) and the symmetry equivalent and "edge-sharing" (vide supra) Pr(2) and Pr(2A) are nine coordinate, each with one Pr−N and eight Pr−Se bonds that average 2.75(4) and 3.08(9) Å, respectively. The outer Pr(3) and Pr(4) are eight coordinate, with two Pr−N and six Pr−Se bonds that average 2.67(3) and 3.00(6) Å, respectively. There are five different types of selenido bridges in the structure: two μ_5-Se^{2-}, one μ_3-Se^{2-}, five μ_2-$(Se_2)^{2-}$, one μ_3-$(Se_2)^{2-}$, and two μ_4-$(Se_3)^{2-}$ with fairly consistent Se−Se distances that average 2.38(1) Å. The one μ_3-selenido anion that bridges two nine-coordinate Pr and the terminal Hg(SePh) is part of the (Se)Hg(SePh) capping group, including that group's disorder about the crystallographic 2-fold axis. Comparisons to related bond lengths in the Cambridge Structural Database (CSD) appear most appropriate when considering the bonds from Ln to the different Se-containing ligands, e.g., Se, Se_2, Se_3, and SePh. In the structure of **2**, there are two symmetry equivalent Se that bridge five Pr atoms with a 2.97−3.10 Å range of Pr−Se distances, which is a rather wide range compared to the 7 structures in the CSD, whose Ln−Se distances (Ln = Nd, Sm, Pr, Ce) for 5-coordinate Se range from 3.01 to 3.03 Å (3.01−3.19 Å if Cp*-containing structures are included).[4c,10b,10c] The wider range in **2** reflects the several different Pr *and* Se coordination environments. For the Pr bonded to the Se_3 ligand, there is one similar precedence[10a] (Ln = Sm) in which there were two shorter Sm−Se (2.96 and 3.01 Å) and one longer, central Sm−Se bond length (3.20 Å). These compare well with the respective Pr−Se values here of 3.02, 3.02, and 3.11 Å; the latter distance, Pr(1)−Se(3), is significantly shorter than the other Pr−Se(3) distance, namely, Pr(2)−Se(3) at 3.29 Å. This distinctive interatomic separation emphasizes the useful characterization of the Pr(1)−Se_6 moiety as a face-capping group. There are 14 structures[10b,c,19−22] in the CSD with the diselenide linkage, namely, Ln−Se_2−Ln, with a range of 2.76−3.01 Å for Ln = Sm, Nd, Yb, Er, Ho, and Tm (mean 2.86(2) Å). These values are shorter than those for the 6 similar linkages in **2**, where the range is 2.94−3.15 Å (mean 3.00(6) Å), likely due to strain in the coordination spheres of Pr(2) and Pr(2A), which are on edge-sharing sites of two $Pr_4(Se_2)_4$ squares (see Figure 1). Also, Pr is a larger Ln than most of this CSD group, and so its bond lengths are expected to be somewhat longer. The last two Se bridging sites to describe in the structure of **2** have bonds to Hg(1), and there are 5 structures[5d,23b,23c] in the CSD with similar Ln−Se−Hg−SePh connectivity found in **2**. However, the bond lengths in **2** involving Hg are significantly shorter than those in the five CSD structures. In the CSD, the Ln−Se bond lengths (Ln = Eu, Sm, Er, Yb) have a range of 2.74−3.23 Å (mean 3.03(2) Å), the Se−Hg bond lengths have a range of 2.57−2.97 Å (mean 2.76(2) Å), and the Hg−Se(Ph) bond lengths have a range of 2.51−2.92 Å (mean 2.63(2) Å). For **2**, these values are 3.008(2), 2.478(8), and 2.446(5) Å, respectively, for Pr(2)−Se(11)−Hg(1)−Se(12), as in Figure 1. Although the Pr−Se is close to the CSD average in this case, the Hg−selenido and Hg−selenolate bond distances are significantly shorter in **2**. This is likely due to the fact that the Hg in the CSD structures[22] are also formally bonded to two additional Se atoms in one "corner" of a cubane-like motif, whereas the Hg in **2** has a flatter coordination environment and is rather remotely associated with the two Se atoms perpendicular to the Pr(2)−Se(11)−Hg(1)−Se(12) extended group as characterized by the distances Hg(1)−Se(5) and Hg(1)−Se(10) of 3.073(3) and 3.210(3) Å, respectively.

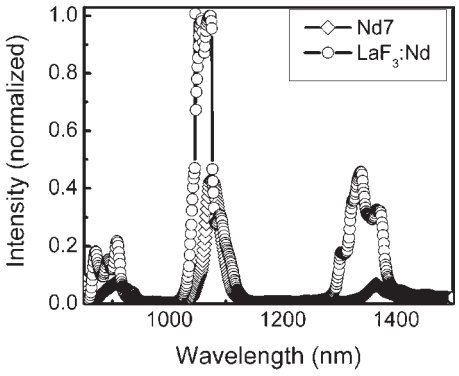

Figure 2. Near-infrared emission spectra of $(py)_{11}Nd_7Se_{21}$(HgSePh) and 0.5 mol % Nd-doped LaF_3.

Incorporation of Hg(II) into the product is consistent with earlier attempts to prepare heterometallic Ln−main group chalcogenido cluster compounds,[23] where a large excess of Ln leads to discrete heterometallic products rather than the charge-separated products that are frequently observed[24] whenever an excess of M is available to abstract EPh. Ionic structures are also disfavored by the excess Se, because the Ln−Se^{2-} bonds are electrostatically stronger than are Ln−SePh bonds and so are less likely to form ionic species

Thermolysis of the Pr compound **2** at 650 °C for 5 h gave a product whose X-ray powder diffraction profile was used to identify both Pr_3Se_4[18] and Pr_2Se_3[17] phases. The solid-state mixture of metallic Pr_3Se_4 and semiconducting Pr_2Se_3 are known and require a much higher (1645 °C) temperature for solid-state preparation.[25] Contents of the cold part of the tube were identified by GC/MS spectroscopy as $SePh_2$.

The potential utility of clusters as signal amplifiers[6] in polymer optical fibers[26] continues to motivate our interest in characterizing and understanding cluster emission properties. The absorption spectrum of **3** (see Supporting Information) displays the spectral transitions and absorbance typical of Nd^{3+} in solid-state materials.[27] Judd−Ofelt parameters were extracted[28] from the absorption spectrum to calculate radiative lifetime (τ_{rad}). A value of 1209 μs was obtained for absorbance leading to the 1075 nm $^4F_{3/2} \rightarrow {}^4I_{11/2}$ emission.

The emission spectrum was experimentally obtained by exciting the metastable level $^4F_{3/2}$ with 800 nm light. Figures 2 and 3 show the near-infrared and short-wavelength infrared emission spectra for Nd7 with reference to 0.5 mol % Nd-doped

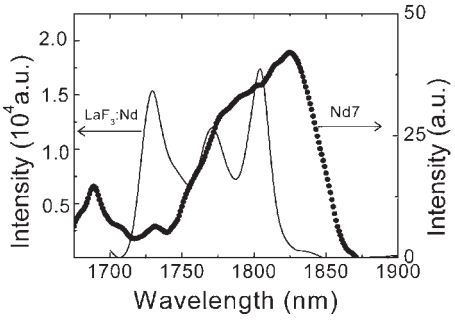

Figure 3. Short-wavelength infrared emission spectra of $(py)_{11}Nd_7Se_{21}(HgSePh)$ and 0.5 mol % Nd-doped LaF_3.

Table 2. Neodymium Compounds with the Highest Quantum Efficiencies

compound/material	QE	ref
nanoscale Nd_2O_3	5×10^{-3}	34
$Nd(pos)_3$	3.3	30
$(DME)_2Nd(SeC_6F_5)_3$	9	4c
$(py)_{18}Nd_{12}O_6(SeSe)_4(SePh)_4$...	12	5c
$(THF)_8Nd_8O_2Se_2(SePh)_{16}$	16	4c
$(py)_xNd_{17}Se_{17}Na(SePh)_{18}$	35	5b
$(py)_{24}Nd_{28}F_{63}(SePh)_{16}$	41	5a
$(py)_{11}Nd_7Se_{21}HgSePh$	43	this work
solid-state Nd:LaF_3 (0.5 mol % Nd)	95	31b
solid-state Nd:La_2Se_3 (1.3 mol % Nd)	100	32

LaF_3. As found in Nd-doped solid-state materials, emission bands were observed at 907, 1075, 1364, and 1824 nm corresponding to the $^4F_{3/2} \rightarrow {}^4I_{9/2}$, $^4F_{3/2} \rightarrow {}^4I_{11/2}$, $^4F_{3/2} \rightarrow {}^4I_{13/2}$, and $^4F_{3/2} \rightarrow {}^4I_{15/2}$ transitions, respectively. However, emission intensities for solid-state materials were consistently much brighter than compound **3**. The fluorescence branching ratios for these transitions were found to be 13%, 69%, 16%, and 2% for the 907, 1075, 1364, and 1824 nm emission bands, respectively.

It is interesting to note that in compound **3** the $^4F_{3/2} \rightarrow {}^4I_{15/2}$ transition is also observed at room temperature. This relatively low-energy (1.8 μm) transition is extremely unusual. This transition has been observed in solid-state fluorides,[31] sulfides,[32] selenides,[33] and tellurite glasses,[34] all of which are considered low-phonon host environments. Similarly, in molecular systems this transition has also been observed in compounds that contain primarily chalcogen-based anions (i.e., $(DME)_2Nd(SC_6F_5)_3$,[4c] $(THF)_8Nd_8O_2Se_2(SePh)_{16}$,[4c] and $(py)_{17}Nd_{17}NaSe_{16}(SePh)_{18}$[5b] but not in either the related phenoxide $Nd(OC_6F_5)_3$[3] or the chalcogen-encapsulated $Nd_{12}O_6$ and $Nd_{28}F_{63}$[5a] clusters.[5c] The low-phonon characteristic of the chalcogenido ligands is clearly crucial to the observation of this particularly low-energy emission.

In order to measure the intrinsic quantum efficiency of the $^4F_{3/2} \rightarrow {}^4I_{11/2}$ transition (1075 nm emission), the fluorescence decay time (τ_{fl}) was extracted from the measured decay curve shown in the Supporting Information. The decay curve was fitted with a Monte Carlo model[29] to yield a decay time of 520 μs for the 1075 nm emission. The fitting takes into account all of the cooperative energy transfer and cross-relaxation processes between Nd atoms located in the various crystallographic sites. The experimental decay time, together with the calculated radiative decay time, results in a calculated quantum efficiency of 43% for **3**.

This is currently the highest quantum efficiency reported for a 'molecular' Nd compound. Table 2 lists the efficiencies of Nd compounds containing E-based ligands that have been analyzed to date, along with data for more conventional molecular sources (i.e., Nd(bis(perfluorooctylsulfonyl)aminate)$_3$, or Nd-(pos)$_3$)[30] and Nd-doped solid-state materials. While solid-state materials still exhibit much higher quantum efficiency (e.g., 100%), the only molecular compound that is similar is our work on $(py)_{24}Nd_{28}F_{63}(SePh)_{16}$, which has a reported quantum efficiency of 41%.[5a] On the basis of inherent error in computing quantum efficiency (10−20%), these compounds are statistically similar and our result with our Nd7 compound is an indication that there is an opportunity to make compounds that have comparable if not even higher quantum efficiency. Examining all the compounds listed in Table 2, even after factoring in the maximum possible experimental error, it is clear the molecular compounds containing chalcogen-based anions enhance NIR emission in a significant fashion. There are two reasons why these compounds show enhanced emission, which we discussed in previous papers. First, the low-energy Ln−E stretching frequencies couple inefficiently with excited-state Ln ions. Second, the longer Ln−E bond length displaces the vibronically active C−H bonds further from the Ln ion than did any of the more traditional ligands reported prior to our work. The recent description of the larger nanoscale Nd17 cluster showed that increasing the size of an emissive cluster increases quantum efficiency because it lowers the relative concentration of fluorescence quenching C−H groups. The Nd7 compound described here is consistent with previous measurements in that it is the most efficient cluster reported to date, and it also has the smallest ratio of C−H bonds/Nd ions. To improve emission efficiency further, we can consider reducing the number of CH bonds by increasing the size of the cluster molecule, deuterating the pyridine, or chemically displacing the remaining SePh ligand with an additional polyselenide ligand.

CONCLUSION

Lanthanide polyselenide clusters can be prepared in high yield by ligand-based reduction of Se with $Ln(SePh)_3$, and they can be converted thermally to a mixture of solid-state phases including Ln_3Se_4. Spectroscopic analysis of the Nd cluster shows that combination of a low-phonon selenide environment and distancing the C−H bonds further from the Nd leads to high-NIR quantum efficiency, with Nd7 having the highest quantum efficiency reported to date. Most important, the gamut of work done so far suggests that these structural features lay the groundwork for families of molecular luminescent compounds that have comparable behavior to solid-state materials.

ASSOCIATED CONTENT

Supporting Information. X-ray crystallographic files in CIF format for the crystal structures of **1**, **2**, and **3**; absorption spectra for **3**; emission decay curve for the 1075 nm transition for **2**; XRPD profile for the solid products formed in the thermolysis of **3**. This material is available free of charge via the Internet at http://pubs.acs.org.

dx.doi.org/10.1021/ic201509v |*Inorg. Chem.* 2011, 50, 9184–9190

AUTHOR INFORMATION

Corresponding Author
*E-mail: bren@rci.rutgers.edu.

ACKNOWLEDGMENT

J.G.B. acknowledges support from the NSF (CHE-0747165); R.E.R., M.R., and G.A.K. acknowledge support from the Defense Advanced Research Project Agency (ONR N00014-08-1-0131).

REFERENCES

(1) Hebbink, G. A.; Reinhoudt, D. N.; van Veggel, F. C. J. M. *Eur. J. Org. Chem.* **2001**, 4101. (b) Hasegawa, T.; Ohkubo, K.; Sogabe, Y.; Kawamura, Y.; Wada, N.; Nakashima, S.; Yanagida *Angew. Chem.* **2000**, *112*, 365. (c) Van Deun, R.; Nockemann, P.; Görller-Walrand, C.; Binnemans, K. *Chem. Phys. Lett.* **2004**, *397*, 447.

(2) (a) Rusakova, N. V.; Topilova, Z. M.; Meshkova, S. B.; Lozinskii, M. O.; Gevaza, Y. I. *Russ. J. Inorg. Chem.* **1992**, *37*, 116. (b) Hasegawa, K.; Murakoshi, Y.; Wada, S.; Yanagida, J.-H.; Kim, N.; Nakashima, C.; Yamanaka *Chem. Phys. Lett.* **1996**, *248*, 8. (c) Batista, H. J.; De Andrade, A.; Longo, R. L.; Simas, A. M.; De Sa, G. F.; Ito, K. N.; Thompson, L. C. *Inorg. Chem.* **1998**, *37*, 3542. (d) Chauvin, A.; Gumy, F.; Matsubayashi, I.; Hasegawa, Y.; Bünzli, J. C. G. *Eur. J. Inorg. Chem.* **2006**, 473. (e) Glover, P. B.; Bassett, A. P.; Nockemann, P.; Kariuki, B. M.; Van Deun, R.; Pikramenou, Z. *Chem.—Eur. J.* **2007**, *13*, 6308.

(3) Norton, K.; Kumar, G. A.; Dilks, J. L.; Emge, T. J.; Riman, R. E.; Brik, M. G.; Brennan, J. G. *Inorg. Chem.* **2009**, *48*, 3573.

(4) (a) Banerjee, S.; Kumar, G. A.; Emge, T. J.; Riman, R. E.; Brennan, J. G. *Chem. Mater.* **2008**, *20*, 4367. (b) Kumar, G. A.; Kornienko, A.; Banerjee, S.; Riman, R. E.; Emge, T. J.; Brennan, J. G. *Chem. Mater.* **2005**, *17*, 5130. (c) Banerjee, S.; Huebner, L.; Romanelli, M. D.; Kumar, G. A.; Riman, R. E.; Emge, T. J.; Brennan, J. G. *J. Am. Chem. Soc.* **2005**, *127*, 15900. (d) Kornienko, A.; Kumar, G. A.; Riman, R. E.; Emge, T. J.; Brennan, J. G. *J. Am. Chem. Soc.* **2005**, *127*, 3501. (e) Kumar, G. A.; Riman, R. E.; Diaz Torres, L. A.; Banerjee, S.; Romanelli, M. D.; Emge, T. J.; Brennan, J. G. *Chem. Mater.* **2007**, *19*, 2937.

(5) (a) Romanelli, M. D.; Kumar, G. A.; Riman, R. E.; Emge, T. J.; Brennan, J. G. *Angew. Chem.* **2008**, *47*, 6049. (b) Moore, B. F.; Kumar, G. A.; Tan, M. C.; Kohl, J.; Riman, R. E.; Brik, M.; Emge, T. J.; Brennan, J. G. *J. Am. Chem. Soc.* **2011**, *132*, 373. (c) Banerjee, S.; Kumar, G. A.; Riman, R.; Emge, T. J.; Brennan, J. *J. Am. Chem. Soc.* **2007**, *129*, 5926. (d) Kornienko, A.; Banerjee, S.; Kumar, G. A.; Riman, R. E.; Emge, T. J.; Brennan, J. G. *J. Am. Chem. Soc.* **2005**, *127*, 14008.

(6) Kumar, G. A.; Riman, R. E.; Chen, S.; Smith, D.; Ballato, J.; Banerjee, S.; Kornienko, A.; Brennan, J. G. *Appl. Phys. Lett.* **2006**, *88*, 91902.

(7) (a) Fenske., D.; Anson, C. E.; Eichhoefer, A.; Fuhr, O.; Ingendoh, A.; Persau, C.; Richert, C. *Angew. Chem., Int. Ed.* **2005**, *44*, 5242. (b) Eichhoefer, A.; Olkowska-Oetzel, J.; Fenske, D.; Fink, K.; Mereacre, V.; Powell, A. K.; Buth, G. *Inorg. Chem.* **2009**, *48*, 8977. (c) Anson, C.; Eichhoefer, A.; Issac, I.; Fenske, D.; Fuhr, O.; Sevillano, P.; Persau, C.; Stalke, D.; Zhang, J. *Angew. Chem., Int. Ed.* **2008**, *47*, 1326. (d) Fenske, D.; Langetepe., T. *Angew. Chemie, Int. Ed.* **2002**, *41*, 300. (e) Pfistner, H.; Fenske, D. *Z. Anorg. Allg. Chem.* **2001**, *627*, 575. (f) Ahlrichs, R.; Besinger, J.; Eichhofer, A.; Fenske, D.; Gbureck, A. *Angew. Chemie, Int. Ed.* **2000**, *39*, 3929. (g) Zhu, N.; Fenske, D. *J. Chem. Soc., Dalton Trans.: Inorg. Chem.* **1999**, 1067. (h) Fenske, D.; Bettenhausen, M. *Angew. Chem., Int. Ed.* **1998**, *37*, 1291. (i) Behrens, S.; Bettenhausen, M.; Deveson, A. C.; Eichhoefer, A.; Fenske, D.; Lohde, A.; Woggon, W. *Angew. Chem., Int. Ed.* **1996**, *35*, 2215.

(8) (a) Shields, A. J. *Nat. Photonics* **2007**, *1*, 215. (b) Nozik, A. J. *Chem. Phys. Lett.* **2008**, *457*, 3. (c) Rafailov, E. U.; Cataluna, M. A.; Sibbett, W. *Nat. Photonics* **2007**, *1*, 395. (d) Norris, D. J.; Bawendi, M. G.; Brus, L. E.. *Mol. Electron.* **1997**, 281. (e) Heath, J. R. *Chem. Soc. Rev.* **1998**, *27*, 65.

(9) (a) Fenske, D.; Adel, J.; Dehnicke, K. *Z. Naturforsch., B* **1987**, *42*, 931. (b) Kolis, J. W. *Coord. Chem. Rev.* **1990**, *105*, 195. (c) Kanatzidis, M. G.; Huang, S. P. *Coord. Chem. Rev.* **1994**, *130*, 509. (d) Dibrov, S. M.; Deng, B.; Ellis, D. E.; Ibers, J. A. *Inorg. Chem.* **2005**, *44*, 3441. (e) Chen, X.; Huang, X.; Li, J. *Inorg. Chem.* **2001**, *40*, 1341. (f) Stevens, R. A.; Raymond, C. C.; Dorhout, P. K. *Angew. Chem., Int. Ed. Engl.* **1995**, *34*, 2509.

(10) (a) Evans, W. E.; Rabe, G. W.; Ziller, J. W.; Doedens, R. J. *Inorg. Chem.* **1994**, *33*, 2719. (b) Evans, W. J.; Rabe, G. W.; Ansari, M. A.; Ziller, J. W. *Angew. Chem.,Int. Ed.* **1994**, *33*, 2110. (c) Cheng, Y.; Jin, G.; Shen, Q.; Lin, Y. *J. Organomet. Chem.* **2001**, *631*, 94.

(11) (a) Pernin, C. G.; Ibers, J. A. *Inorg. Chem.* **1997**, *36*, 3802. (b) Pernin, C. G.; Ibers, J. A. *J. Cluster Sci.* **1999**, *10*, 71.

(12) (a) Freedman, D.; Emge, T. J.; Brennan, J. G. *Inorg. Chem.* **2002**, *41*, 492. (b) Norton, K.; Banerjee, S.; Das, S.; Huebner, L.; Emge, T. J.; Brennan, J. G. *J. Chem. Soc., Dalton Trans.* **2010**, *39*, 6794.

(13) Bruker-ASX. *SADABS, Bruker Nonius area detector scaling and absorption correction*, v2.05; Bruker-AXS Inc.: Madison, WI, 2003.

(14) Sheldrick, G. M. *SHELXS86, Program for the Solution of Crystal Structures*; University of Göttingen: Göttingen, Germany, 1986.

(15) (a) Sheldrick, G. M. *Acta Crystallogr.* **2008**, *A64*, 112. (b) Sheldrick, G. M. *SHELXL97, Program for Crystal Structure Refinement*; University of Göttingen: Göttingen, Germany, 1997.

(16) Graphics programs: ORTEP-3 for Windows: Farrugia, L. J. *J. Appl. Crystallogr.* **1997**, *30*, 565.Burnett, M. N.; Johnson, C. K. ORTEP-III: Oak Ridge Thermal Ellipsoid Plot Program for Crystal Structure Illustrations. Oak Ridge National Laboratory Report ORNL-6895, 1996; Persistence of Vision Pty. Ltd., Persistence of Vision Raytracer (Version 3.6), 2004.

(17) (a) Schneck, C.; Hoess, P.; Schleid, T. *Acta Crystallogr., Sect. E* **2009**, *E65*, i20/1. (b) Kalitin, S. P. *Inorg. Mater. (Engl. Transl.)* **1965**, *1*, 42.

(18) Dernier, P. *J. Solid State Chem.* **1975**, *15*, 203.

(19) Jin, G.-X.; Cheng, Y.; Lin, Y. *Organometallics* **1999**, *18*, 947.

(20) Evans, W. J.; Nyce, G. W.; Clark, R. D.; Doedens, R. J.; Ziller., J. W. *Angew. Chem., Int. Ed.* **1999**, *38*, 1801.

(21) (a) Kornienko, A. Y.; Emge, T. J.; Brennan, J. G. *J. Am. Chem. Soc.* **2001**, *123*, 11933. (b) Huebner, L.; Kornienko, A.; Emge, T. J.; Brennan, J. G. *Inorg. Chem.* **2005**, *44*, 5118.

(22) (a) Kornienko, A.; Melman, J. H.; Hall, G.; Emge, T. J.; Brennan, J. G. *Inorg. Chem.* **2002**, *41*, 121. (b) Fitzgerald, M.; Emge, T. J.; Brennan, J. G. *Inorg. Chem.* **2002**, *41*, 3528.

(23) (a) Banerjee, S.; Sheckelton, J.; Emge, T. J.; Brennan, J. G. *Inorg. Chem.* **2010**, *49*, 3573. (b) Lee, J. S..; Emge, T. J.; Brennan, J. G. *Inorg. Chem.* **1997**, *36*, 5064. (c) Berardini, M.; Emge, T.; Brennan, J. *Inorg. Chem.* **1995**, *34*, 5327. (d) Berardini, M.; Emge, T.; Brennan, J. *J. Am. Chem. Soc.* **1994**, *116*, 6941. (e) Brewer, M.; Lee, J.; Brennan, J. G. *Inorg. Chem.* **1995**, *34*, 5919.

(24) (a) Banerjee, S.; Emge, T. J.; Brennan, J. G. *Inorg. Chem.* **2004**, *43*, 6307. (b) Freedman, D.; Emge, T. J.; Brennan, J. G. *J. Am. Chem. Soc.* **1997**, *119*, 11112. (c) Kornienko, A.; Huebner, L.; Freedman, D.; Emge, T.; Brennan, J. *Inorg. Chem.* **2003**, *42*, 8476.

(25) Fang, C. M.; Meetsma, A.; Wiegers, G. A. *J. Alloys Compd.* **1995**, *218*, 224.

(26) (a) Kuriki, K.; Kobayashi, T.; Imai, N.; Tamura, T.; Nishihara, S.; Tagaya, A.; Koike, Y.; Okamoto, Y. *IEEE Photonics Technol. Lett.* **2000**, *12*, 989. (b) Xu, X. *Opt. Commun.* **2003**, *225*, 55. (c) Zheng, Z; Liang, H; Ming, H; Zhang, Q; Xie, J. *Opt. Commun.* **2004**, *233*, 149. (d) Liang, H; Zheng, Z; Chen, B; Zhang, Q; Ming, H. *Mater. Chem. Phys.* **2004**, *86*, 430. (e) Kuriki, K; Nishihara, S; Nisizawa, Y; Yosinaga, T; Tagaya, A; Koike, Y; Okamoto, Y. *Opt. Lett.* **2003**, *28*, 570. (f) Liang, H; Zhang, Q; Zheng, Z; Ming, H; Li, Z; Xu, J; Chen, B; Zhao, H. *Opt. Lett.* **2004**, *29*, 477.

(27) (a) Oczko, G. *J. Alloys Compd.* **2000**, *300*, 414. (b) Lis, S. *J. Alloys Compd.* **2000**, *300*, 88. (c) Gubina, K. E.; Shatrava, J. A.; Ovchynnikov, V. A.; Amirkhnov, V. M. *Polyhedron* **2000**, *19*, 2203. (d) Legendziewicz, J.; Oczko, G.; Wiglusz, R.; Amirkhanov, V. *J. Alloys Compd.* **2001**, *323*, 792.

(28) (a) Judd, B. R. *Phys. Rev B.* **1962**, *127*, 750. (b) Ofelt, G. S. *J. Chem. Phys.* **1962**, *37*, 511.
(29) Díaz Torres, L. A.; Barbosa-Garcia, O.; Meneses-Nava, M. A.; Struck, C. W.; Di Bartolo, B. In *Advances in Energy Transfer Processes*; Di Bartolo, B., Chen, X., Eds.; World Scientific Publishing Co.: Singapore, 2000; pp 523−552.
(30) Hasegawa, H; Okhubo, T.; Sogabe, K.; Kawamura, Y.; Wada, Y.; Nakashima, N.; Yanagida, S. *Angew. Chem., Int. Ed.* **2000**, *39*, 357.
(31) (a) Davey., S. T.; France., P. W. *Br. Telecom Tech. J.* **1988**, *7*, 58. (b) Kumar, G. A.; Chen, C. W.; Riman, R. E.. *Chem. Mater.* **2007**, *19*, 1523. (c) Stouwdam, J. W; van Veggel, F. C. J. M. V. *NanoLett.* **2002**, *2*, 733. (d) Shen, S.; Jha, A.; Zhang, E.; Wilson, S. J. *C. R. Chim.* **2002**, *5*, 921. (e) Payne, S. A.; Bibeau, C. *J. Lumin.* **1998**, *79*, 143.
(32) Schweizer, T. Ph.D. Thesis, Universitat Hamburg, 1998
(33) In *Optical Fiber Amplifiers-Materials, Devices, and Applications*; Sudo, S., Ed.; Artech House Inc.: Norwood, MA, 1997.
(34) Shen, S.; Jha, A.; Zhang, E.; Wilson, S. J. *C. R. Chim.* **2002**, *5*, 921.
(35) Bazzi, R.; Brenier, A.; Perriat, P.; Tillemenet, O. *J. Lumin.* **2005**, *113*, 161.